Available online at www.sciencedirect.com
ScienceDirect
Materials Chemistry and Physics 103 (2007) 305–311
MATERIALS CHEMISTRY AND PHYSICS
www.elsevier.com/locate/matchemphys

Structural studies on vacuum evaporated ZnSe/p-Si Schottky diodes

S. Venkatachalam [a], D. Mangalaraj [a,*], Sa.K. Narayandass [a], S. Velumani [b], P. Schabes-Retchkiman [c], J.A. Ascencio [d]

[a] *Thin Film Laboratory, Department of Physics, Bharathiar University, Coimbatore, India*
[b] *Departamento de Fisica, ITESM-Campus Monterrey, E.Garza Sada, #2501 Monterrey, Nuevo Leon, C.P. 64849, Mexico*
[c] *Instituto de Física, University Nal. Autónoma de México, A. P. 20-364, C.P. 01000 México, D.F., Mexico*
[d] *Instituto Mexicano del Petroleo, Eje Central Lazaro Cardenas, 152 Mexico, D.F. 07730, Mexico*

Received 6 February 2006; received in revised form 26 December 2006; accepted 19 February 2007

Abstract

ZnSe/Si heterostructures, fabricated by vacuum evaporation method, are investigated by Rutherford backscattering spectrometry (RBS), X-ray diffraction (XRD), optical, *I–V*, *C–V* analysis, high-resolution electron microscopy (HREM) and ab initio quantum mechanics calculations. From the RBS analysis, the composition of the deposited film is found to be nearly stoichiometric. The structural studies show that the orientation of the crystallites in the deposited film is along (1 1 1) direction. Particle size (D), strain (ε) and dislocation density (δ) values are calculated as 40.71 nm, 0.95×10^{-3} lin^{-2} m^{-4} and 6.03×10^{15} lin m^{-2}, respectively, while ZnSe/Si interface was locally studied to establish the high interaction between both crystals and it clears that the Si order produce the gradual array in the ZnSe crystallization. The optical band gap value of the deposited films is calculated as 2.61 eV. The ideality factor is evaluated from the *I–V* measurement and its value is found to be in the range of 2.8–3.01. From the *C–V* analysis, the built in potential is found to be 0.61 V. The value of effective carrier concentration (N_A) and the barrier height are determined as 3.8×10^{11} cm^{-3} and 1.457 eV, respectively.

Keywords: Thin films; ZnSe/Si Schottky diodes; RBS; XRD; Optical; HREM and ab initio quantum mechanics

1. Introduction

II–VI compounds have been considered as promising materials for application in many areas of recent development. Recently, the hetero-structures based wide-band gap II–VI compound semiconductors have attracted much attention because of their properties and their applicability in laser diodes [1] and in several types of optoelectronic devices [2]. In particular, the ZnSe/Si heterojunction is of specific interest since this structure provides effective solar cells with efficiencies of 17.5% [3] and enables the integration of wide bandgap device in silicon circuits. Because of the difference in physical parameters such as lattice constants, thermal expansion coefficients and ionicity between ZnSe and Si, this material system suffers from a number of crystalline defects, which have a deleterious effect on the optical and electronic properties and may be responsible for the reduction of the device lifetime [4,5]. The crystallographic quality of thin films largely depends on the ambient pressure and lattice match [6]. The lattice mismatch between ZnSe and GaAs is quite small (0.27%), but the lattice mismatch between ZnSe and Si is quite large (4.4%). Thus, the application in optoelectronic devices has increased the need for a better knowledge on the defect structure of this material system, basically the effect of the Si crystalline order on the cluster formation of ZnSe and the scale range of interaction to the thin film formation. The thermal expansion coefficient is greatly reduced by incorporation of iodine in ZnSe compound, and also the outermost electrons of iodine atoms with large ionic radius are easily polarizable. The n-type doping of I_{Se} gives rise to the stabilization of ionic charge distributions due to decrease in Madelung energy [7]. Hence an attempt has been made on the preparation of Si based ZnSe heterostructure using the iodine doped ZnSe compound.

During the last few decades the use of both, experimental and theoretical methods together have produced more knowledge on the basis to generate a material and the effects of the structure on its corresponding properties [8], since the nanostructured [9–11] to the bulk-like structures [12,13]. Particularly the case

* Corresponding author. Tel.: +91 422 2425458; fax: +91 422 2422387.
E-mail addresses: dmraj800@yahoo.com (D. Mangalaraj), ascencio@imp.mx (J.A. Ascencio).

0254-0584/$ – see front matter © 2007 Elsevier B.V. All rights reserved.
doi:10.1016/j.matchemphys.2007.02.077

of the basis for nanostructured arrays and crystalline interfaces have received an important impulse to molecular simulation approaches, which allow understanding how the local atomic distribution induce the trybological and mechanical behaviour of the whole system [14].

In this paper, we report a hybrid study involving the experimental characterization of the composition, structural and optical properties, besides atomistic and electronic studies with help of quantum mechanics based methods for ZnSe thin films along with the formation of ZnSe/p-Si Schottky hetrostructure and the junction parameters like built in potential (V_{bi}), $V_{n,}$ N_v the density of states in the valance band, ϕ_{Bn}.

2. Experimental methods and theoretical approaches

2.1. Sample preparation

The ZnSe compounds were prepared at 875 °C with iodine as a reactive doping agent. ZnSe thin films were deposited onto the well cleaned glass and Si (1 0 0) substrates at a substrate temperature of 589 K under a vacuum of 3×10^{-5} Torr and Au was used as top electrode. The complete device had an active area of 3×10^{-6} m^2. The composition of the film deposited onto silicon substrate is studied using Rutherford backscattering spectrometry. 2 MeV He^+ ion beam was used for the experiment. The details of the experimental set-up can be found elsewhere [15]. The RBS analysis was performed using a simulation code Rump [16]. X-ray diffractometer (Philips PW 1700) with Ni-filtered Cu Kα radiation (λ = 1.54056 Å) was used to study the structural properties of the films. The optical transmittance spectra were recorded using a UV–vis–NIR spectrophotometer (Hitachi, Japan) in the wavelength range from 200 to 2500 nm. The current across the device as a function of the applied voltage from a dc power supply was measured in a rotary vacuum of 1×10^{-2} Torr at different temperatures (309–396 K) using a cryostat equipped with a PT100 thermocouple.

2.2. Structural analysis

The particle size (D) is calculated using the Scherrer formula from the full width at half maximum (β) (FWHM).

$$D = \frac{0.94\lambda}{\beta \cos\theta} \tag{1}$$

where λ is the wavelength of the X-ray used, β the full width at half maximum and θ is the angle between the incident and the scattered X-ray.

The lattice parameter ($h\,k\,l$) is determined by the following expression for cubic structure:

$$\frac{1}{d^2} = \frac{h^2 + k^2 + l^2}{a^2} \tag{2}$$

where h, k, l represent the lattice planes and 'a' the lattice parameter. The strain values (ε) were evaluated by using the following relation:

$$\varepsilon = \left[\frac{\lambda}{D\cos\theta} - \beta\right] \times \frac{1}{\tan\theta} \tag{3}$$

The dislocation density (δ) has been calculated by using the formula (Pradip et al. [17]) for cubic ZnSe thin films

$$\delta = \frac{15\varepsilon}{aD} \tag{4}$$

For nano-characterization we have made use of transmission electron microscopy (TEM), particularly by high resolution, which allows the structural analysis of local arrays in the order of atomic columns and how defects are distributed forming small range arrays; besides high angle annular dark field that allows a kind of Z-contrast to differentiate between different compositions on a sample. These techniques were performed in a JEM 2010 FasTem analytical microscope equipped with a GIF detector. High-resolution images were obtained at the optimum focus condition (Sherzer condition).

Theoretical analysis of the electronic properties were made for a periodic structure of ZnSe and Si separated by using the Castep software [18], which is a ab initio method based on a plane wave approach for crystal models and considering the gradient corrected approximation (GCA) and the Perdew–Burke–Ernzerhof functional [19]. The energetic evaluation of ZnSe/Si was evaluated with the help of a model of ZnSe on a Si surface and studying the stress tensor during a geometry relaxation and the local interaction between Si and ZnSe atoms; it was considered as follows: a convergence tolerance of 5×10^{-6} eV/atom between the steps, a self consistent field tolerance of 5×10^{-7} eV/atom for each single point of energy calculation, and a $9 \times 9 \times 4$ k-point set. Similar calculations by DFT for molecular models were improved by the DMol3 software [20], which allows a similar basis set and a geometry optimization goal. In order to make the calculation and visualization analysis we used the Castep and DMol3 modules of the Cerius^2 software by Accelrys.

3. Results and discussion

Fig. 1 shows a typical RBS spectrum of ZnSe thin films deposited onto the well cleaned Si substrates at 589 K. The RBS spectrum of the deposited film along with a fit is obtained using the simulation code RUMP [16]. This fit shows the contribution of the individual peaks corresponding to the various elements of the RBS spectrum. Starting with the high energy side, we identify peaks corresponding to I, Se, Zn and Si, respectively. The composition of the deposited film is found to be $Zn_{0.5}Se_{0.5}$ and the iodine concentration was found to be almost negligible.

A typical X-ray diffractograms of ZnSe films deposited onto Si substrates at 589 K is shown in Fig. 2. The deposited films have a strongly preferred orientation and only one intense peak was observed. The observed lattice spacing value (d = 3.276 Å) coincides with the reported value of cubic ZnSe. Xu et al. [21] have obtained polycrystalline structure using pure single ZnSe polycrystal target. But we have obtained a very good single phase cubic structure using this synthesized ZnSe compound. The XRD patterns for the deposited films exhibit reflections at 27.14°, corresponding to the cubic phase. Hence the ZnSe films of higher thicknesses deposited in vacuum onto the Si

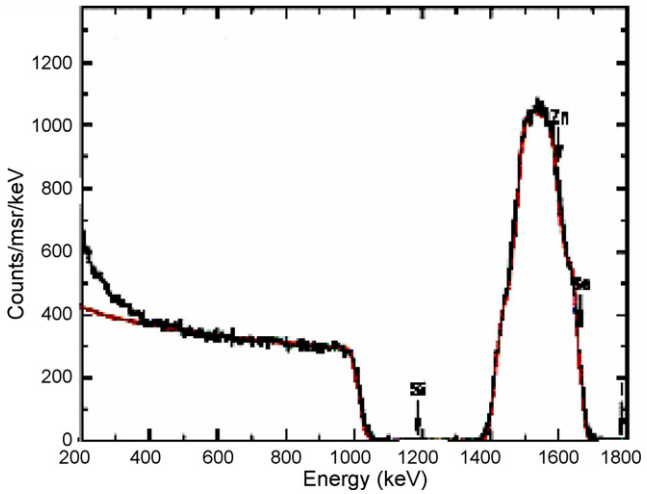

Fig. 1. Rutherford backscattering spectrum of vacuum evaporated ZnSe thin film.

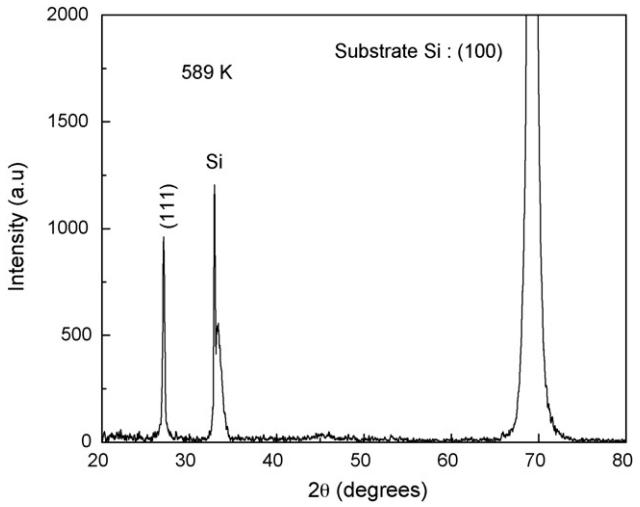

Fig. 2. X-ray diffractogram of ZnSe films deposited onto Si substrate at a substrate temperature of 589 K.

substrates at 589 K found to have more preferred orientation along (1 1 1) direction and are in cubic phase. The evaluated values of particle size, strain, dislocation density and lattice constant values were found to be 40.71 nm, 0.95×10^{-3} lin^{-2} m^{-4}, 6.03×10^{15} lin m^{-2} and 5.681 Å, respectively. The calculated lattice constant value coincides well with the already reported value [22].

Since the crystalline structure identified by the X-ray diffraction (XRD), corresponds to the average of the sample, the use of HREM images allows identifying how the ZnSe has been deposited and what are the main adopted configurations. In Fig. 3, it can be observed the two main types of contrasts identified for the ZnSe in the sample, with long regions of single crystalline structures (Fig. 3a) and small regions with multiple small clusters (Fig. 3b), which suggest the formation of big crystals in some regions of the samples (up to 100 nm) and the multiple defects near to the surface that can be identified as many small aggregates producing a polycrystalline zone with nanograins. In Fig. 3a, the measured lattice spacing matches directly to the ZnSe (0 0 2) plane distances, while the included fast Fourier transform (FFT) pattern allows determining one single orientation and a clean periodicity over the analyzed region. In addition in Fig. 3b, the small nanodomains making a polycrystalline domain, are shown where multiple orientations can be identified as it can be also distinguished from the included FFT pattern.

The effects of these types of structures involve important considerations, however it must be established that the long crystals domains in the samples is more than that 80% of the analyzed regions, while the small grains are basically found nearer to the ZnSe/Si interface. In fact, Fig. 3b allowed identifying two different lattices, as it can be seen from the different distances of the spots marked with the arrow on the FFT, which determines two contributions with different lattice spacing. In this way, the influence of the Si–ZnSe lattice mismatch implies the local effects on the new material formation, and hence, the produced interface must generate defects on the ZnSe film in the short range, making the evaluation of this region a crucial element on the understanding of the obtained material and its performance.

In Fig. 4 a complete analysis of the interface region is made, which has a elemental composition identified for the two different crystals as it can be seen in Fig. 4a, where the X-ray emission signals of Zn, Se and Si, are identified (besides the copper from the grid where the samples are deposited for their analysis). From this region the use of HREM images (Fig. 4b) that it is obtained from the square selected are from the particle distinguished with help of the HAADF image of Fig. 4c, which clearly correspond to the interface of a layer of ZnSe on a Si aggregate. In fact the FFT pattern establishes a polycrystalline sample for two different crystals.

A deeper analysis of the HREM image allows recognizing an interface where the lattice mismatch correspond to that reported in previous works, however the structural homogeneity is of short range and followed by small clusters and deformed clusters. This last effect of local interaction implies that the interface regions control not only the trybological properties of

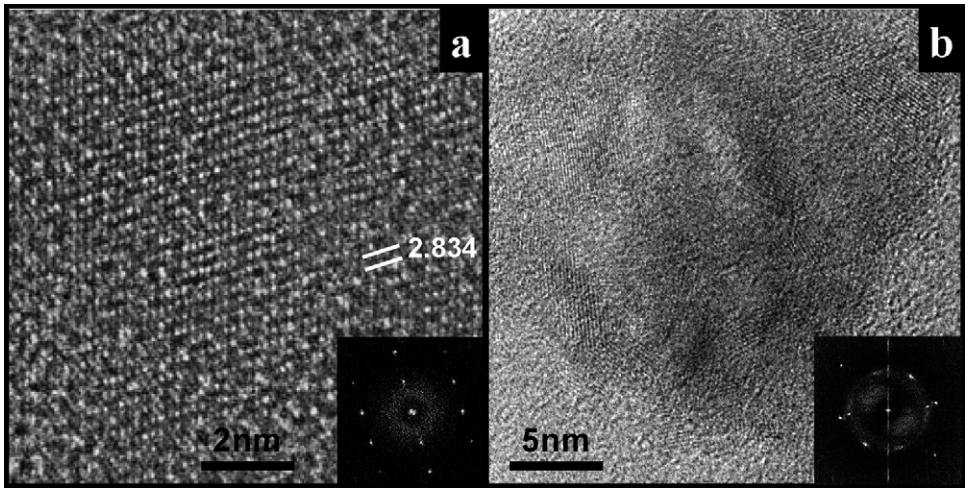

Fig. 3. HREM images from different regions of the samples. (a) A big crystal grain of ZnSe and (b) a multiple domains zone of ZnSe and Si. In both images the corresponding FFT are inset for clarity.

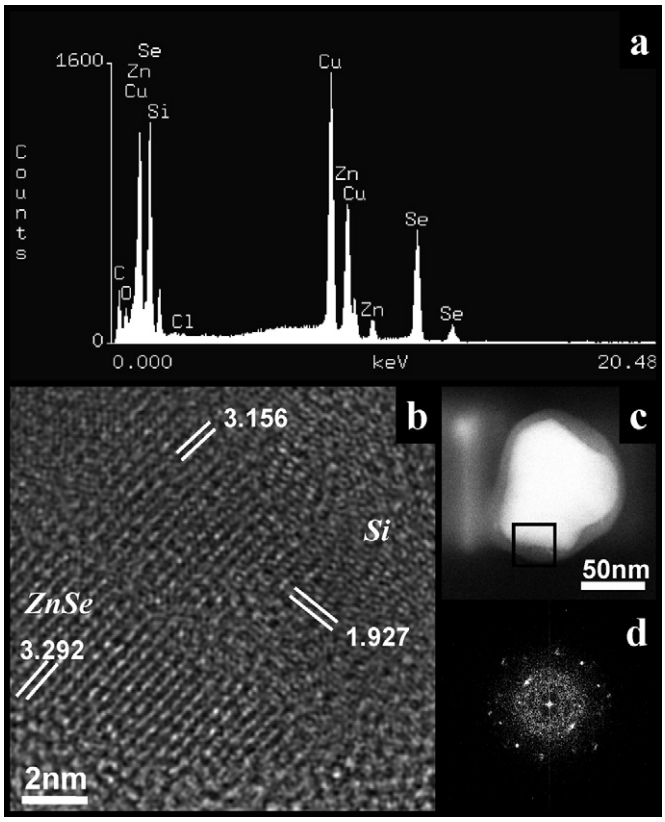

Fig. 4. Transmission electron microscopy analysis of an interface section. (a) EDS elemental composition spectra from the interface region, (b) the corresponding HREM image, (c) HAADF of the whole grain and the corresponding and (d) FFT pattern.

the deposited films, also the structure of the produced material, which will be more deformed if the Si surface is not sufficiently flat.

In order to evaluate the effects of this interaction between the Si surface and the deposited ZnSe, theoretical methods have been used to identify the stress involved as effect of the interface and the density of states for the pure crystals and for the ZnSe/Si diode. In Fig. 5, the results of the quantum mechanical calculation are shown as part of the understanding for the different structures, the pure ZnSe and Si crystals besides the ZnSe/Si interface. The electrostatic iso-surfaces potential are shown for (a) ZnSe, (b) Si and (c) ZnSe/Si, which allows to identify the Zn atoms domain in the EP distribution in the ZnSe crystal, for the Si, there is an homogeneous distribution and when both crystals are together the Se presents in a low contribution in the surfaces.

The densities of states (DOS) plot for the different crystals are also shown in Fig. 5d, where it is clear that the junction induce better localized regions for most of the electrons reducing the band gap. Besides the geometry optimization for the model proposed for the ZnSe deposition on the Si surface, is shown in Fig. 5e and f (proposed and relaxed configurations, respectively), where the local deformation of the crystalline order in both materials is clearly shown. The effect of this deformations are also evaluated using the electrostatic iso-surface potential which has been shown in Fig. 5g, denotes a polarization of the surface, which induce small negative regions on the top of the model that implies a lower effect of the interaction while the ZnSe film thickness increases.

The optical transmittance spectrum of ZnSe thin films deposited onto well cleaned glass substrates is shown in Fig. 6 and in the inset is the plot between $(\alpha h\nu)^2$ and $h\nu$ for ZnSe thin film deposited at 589 K. The band gap was obtained by extrapolation of the plot of $(\alpha h\nu)^2$ and $h\nu$, which yields the energy band gap values of ZnSe films. The evaluated band gap value for the film deposited at 589 K was found to be 2.61 eV. Similar results for CBD deposited ZnSe thin films have been reported by Chaudhari et al. [23].

The electrical properties of practical Schottky barrier diodes (SBD) are mainly controlled by the interface properties. Fig. 7 shows the typical plot of current versus voltage characteristic studies of ZnSe/Au Schottky diodes in forward and reverse bias conditions measured at different temperatures. *I–V* characteristics follow the standard diode equation [24]

$$I = I_0 \left[\exp\left(\frac{qV}{nkT} \right) - 1 \right] \tag{5}$$

where k is the Boltzmann constant, n the ideality factor, q the electronic charge and T is the temperature. The ideality factor was determined at various temperatures using the plot between $\ln I$ and V (Fig. 8). The ideality factor remains almost constant (2.8–3.01) in the temperature range of 306–396 K. The value of barrier height was found to increases (1.457–1.711) with the increase of temperature. The calculated value of barrier height at room temperature is coinciding with the previous results reported by Wang et al. [25]. The temperature dependence of the barrier height is due to the fact that the measured current is a combination of the thermionic current and the recombination current. The departure of the ideality factor from unity may be due to the interfacial layer between the metal and the semiconductor [26]. The variation of diode rectification factor γ versus temperature is shown in Fig. 9 and it is, defined as the ratio of the forward to reverse current. Here we measured the diode rectification factor for the prepared ZnSe/Si device at 1 V. The rectification factor has maximum value (0.223×10^3) at room temperature, the rectification factor decreases with the increase in temperature. Similar results are observed by Rakhshani et al. [24].

C–V measurements were made at 306 K and 1 MHz on the ZnSe/Si diode. In Fig. 10, C^{-2} is plotted as a function of voltage. The straight line plot in Fig. 10 implies a similar behaviour of an abrupt heterojunction [27]. The built in potential (V_{bi}) is calculated from the following relation [28]

$$\frac{1}{C^2} = \frac{2(V_{bi} - V)}{q\varepsilon_s N_D} \tag{6}$$

From Eq. (6), the intercept at $1/C^2 = 0$ corresponds to the built-in potential V_{bi}. It is found to be 0.61 V. The value of barrier height [29] can be calculated from the measured value of V_{bi}.

$$\phi_{Bn} = V_{bi} + V_n + \frac{kT}{q} \tag{7}$$

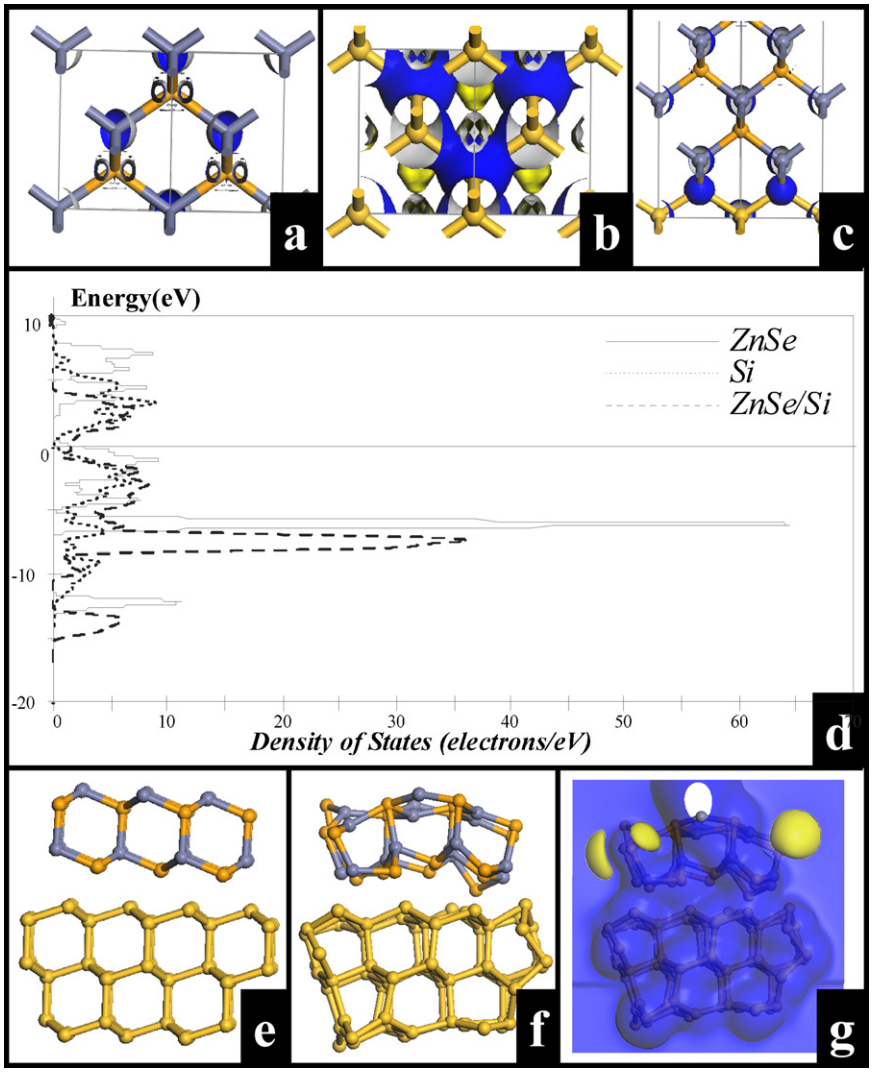

Fig. 5. Quantum mechanical calculation: The electrostatic iso-surfaces potential are shown for (a) ZnSe, (b) Si and (c) ZnSe/Si, (d) the densities of states plot for the different crystals; (e and f) Geometry optimization for the model proposed for the ZnSe deposition on the Si surface, proposed and relaxed configurations, respectively, where the local deformation of the crystalline order in both materials is clearly shown. (g) Electrostatic iso-surface potential denoting a surface polarization.

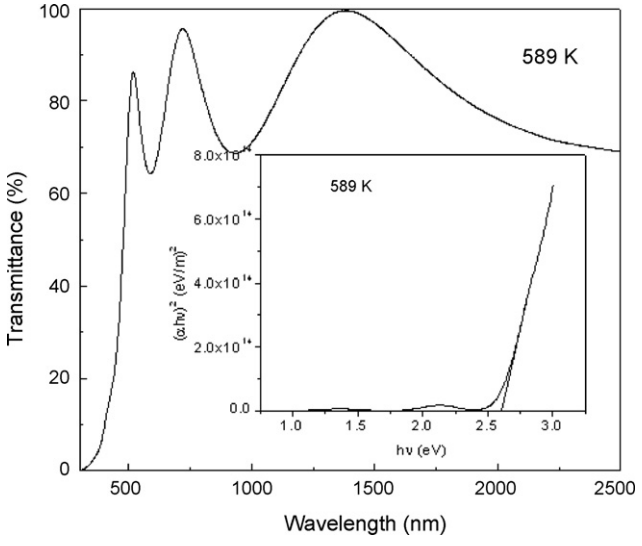

Fig. 6. Transmittance spectra of ZnSe thin film deposited onto glass substrate and inset is the plots of $(\alpha h\nu)^2$ vs. $h\nu$ of ZnSe thin film of thickness 1488 Å deposited onto glass substrate.

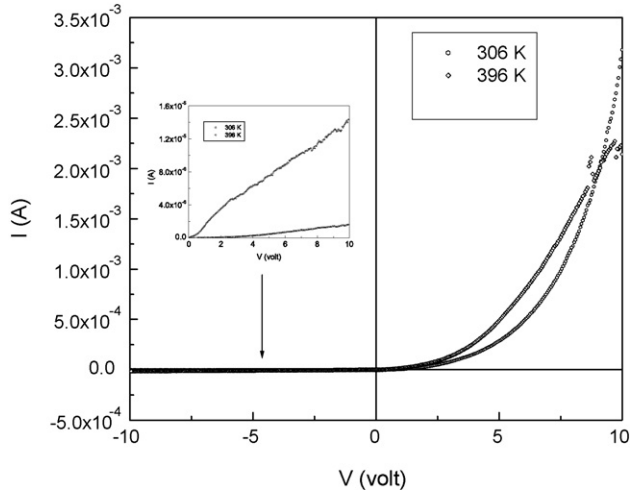

Fig. 7. Forward and reverse current vs. voltage characteristics of ZnSe/Si Schottky diodes.

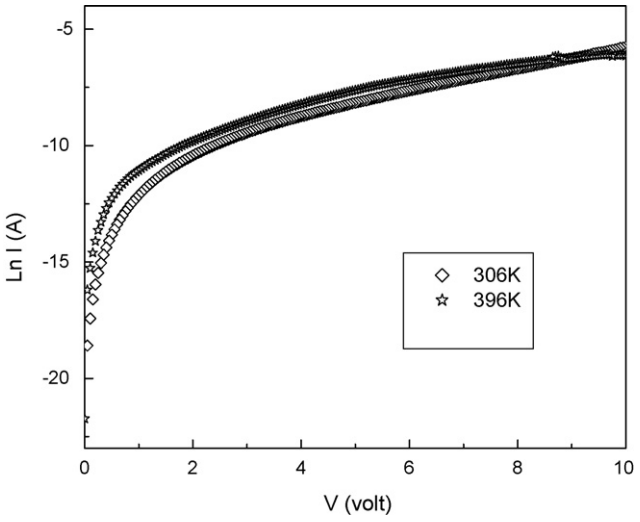

Fig. 8. Variation of ln I vs. voltage characteristics of ZnSe/Si Schottky diodes.

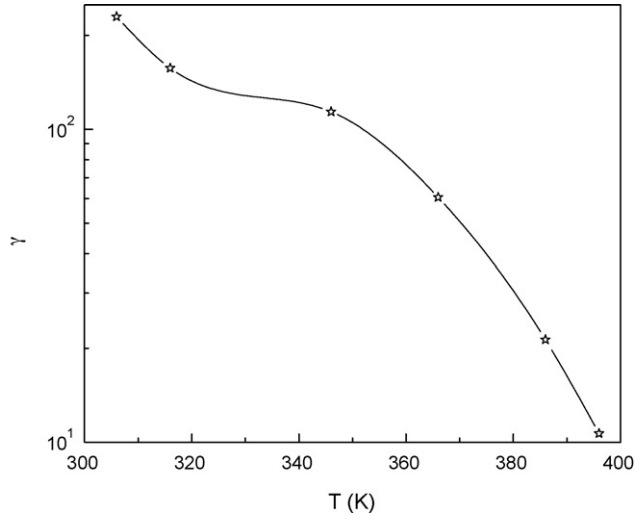

Fig. 9. Temperature dependence of the rectification factor γ for ZnSe/Si Schottky diodes.

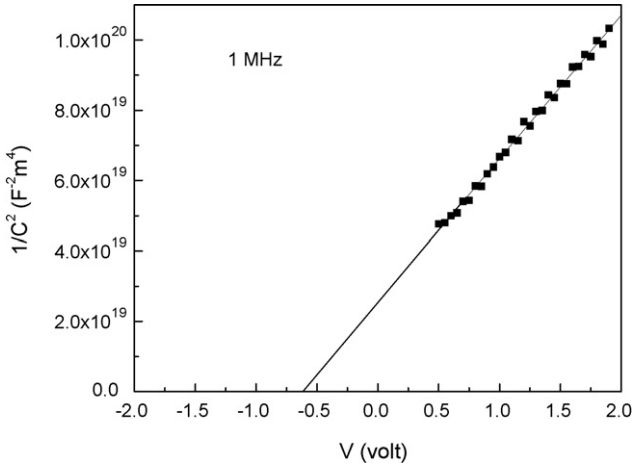

Fig. 10. Dependence of $1/C^2$ value on applied voltage of ZnSe/Si Schottky diodes.

Table 1
The electrical parameters of ZnSe films deposited onto glass substrates

Temperature (K)	306
V_{bi} (V)	0.61
$d(1/C^2)/dV$ ($\times 10^{19}$ $(m^2/F)^2$ V^{-1})	4.083
N_A ($\times 10^{11}$ cm^{-3})	3.8
V_n (V)	0.8202
ϕ_{Bn} (eV)	1.457

where $V_n = kT/q$. $\ln(N_v/N_A)$, k is the Boltmann constant, T the absolute temperature, q the charge of the electron, N_v the density of states in the valance band and N_A is the effective carrier concentration. From the slope of the C^{-2} versus voltage plot, the evaluated N_A and barrier height values were found to be 3.8×10^{11} cm^{-1} and 1.457 eV, respectively. The calculated values of V_{bi}, V_n, N_v and ϕ_{Bn} are given in Table 1 for ready reference.

4. Conclusion

The composition of the simple vacuum deposited ZnSe films is found to be nearly stoichiometric. The effects of the interface are clearly the bigger influence on the thin film structure formation and also, the produced effect directly affects the electronic properties since it was here demonstrated to reduce the band gap in function of the local ZnSe–Si interaction. The small grain production is mainly identified near to the interface what it explained thanks to the quantum mechanical calculations as induced by the crystalline mismatch and the charge density influence between the different elements.

From the optical studies, the transition of the deposited film is found to be direct allowed. The variations of barrier height and ideality factor have been studied as a function of temperature. The SBH of ZnSe/Si has been found to vary between 1.457 and 1.711 eV in the temperature range of 306–396 K. At 306 K, the ideality factor has been found to be 2.8. The C–V analysis reveals the formation of abrupt hetero-junction in the examined ZnSe/Si heterostructure.

References

[1] H. Morkoe, S. Strite, G.B. Gao, M.E. Lin, B. Sverdlow, M. Burns, J. Appl. Phys. 76 (1994) 1363.
[2] R.F.C. Farrow, G.R. Jones, G.H. Williams, I.M. Young, Appl. Phys. Lett. 39 (1981) 954.
[3] A.L. Fahrenbruch, R.H. Bube, Fundamentals of Solar Cells, Academic Press, New York, 1983, p. 302.
[4] S. Guha, J.M. Depuydt, M.A. Haase, J. Qiu, H. Cheng, Appl. Phys. Lett. 63 (1993) 3107.
[5] J.M. Depuydt, M.A. Haase, Guha, J. Qiu, H. Cheng, B.J. Wu, G.E. Hofler, G. Meis-Haugen, M.S. Hagedorn, P.F. Baude, J. Cryst. Growth 138 (1994) 667.
[6] H.B. Boo, N. Xu, J.K. Lee, Vacuum 64 (2002) 145.
[7] Y. Tetsuya, K.-Y. Hiroshi, Jpn. J Appl. Phys. 37 (1998) L910.
[8] G.A. Rosquete-Pina, C. Zorrilla, S. Velumani, J. Arenas-Alatorre, J.A. Ascencio, Appl. Phys. A: Mater. 79 (2004) 1913.
[9] H.B. Liu, G. Canizal, S. Jiménez, M.A. Espinosa, J.A. Ascencio, Comp. Mater. Sci. 27 (2003) 333–341.
[10] V. Lindberg, B. Hellsing, J. Phys.-Condens. Matter 17 (13) (2005) S1075.
[11] R.E. Bailey, S.M. Nie, J. Am. Chem. Soc. 125 (23) (2003) 7100–7106.

[12] A. Boukortt, B. Abbar, H. Abid, M. Sehil, Z. Bensaad, B. Soudini, Mater. Chem. Phys. 82 (3) (2003) 911–920.
[13] J.A. Ascencio, V. Rodrguez-Lugo, C. Angeles, T. Santamara, V.M. Castano, Comp. Mater. Sci. 25 (2002) 413–426.
[14] Z.Q. Liu, A. Neville, R.L. Reuben, Tribol. Trans. 43 (4) (2000) 627–634.
[15] D.N. Jamieson, Nucl. Inst. Meth. B 136–138 (1998) 1.
[16] Doolittle, R. Lawrence, Nucl. Inst. Meth. B 9 (3) (1985) 344.
[17] K.R.L. Pradip, B.K. Sarma, H.L. Das, Bull. Mater. Sci. 23 (4) (2000) 313.
[18] M.D. Segall, P.J.D. Lindan, M.J. Probert, C.J. Pickard, P.J. Hasnip, S.J. Clark, M.C. Payne, J. Phys.-Condens. Matter 14 (11) (2002) 2717–2743.
[19] J.P. Perdew, K. Burke, M. Ernzerhof, Phys. Rev. Lett. 77 (1996) 3865.
[20] B. Delley, J. Chem. Phys. 113 (2000) 7756.
[21] N. Xu, Z.F. Ying, Y.C. Du, F.M. Li, Curr. Appl. Phys. 1 (2001) 209.
[22] Joint Committee on Powder Diffraction Standards, 2000. File No. 37–1463.
[23] G.N. Chaudhari, S. Manorama, V.J. Ral, J. Phys. D: Appl. Phys. 25 (1992) 862.
[24] A.E. Rakhshani, Y. Makdisi, X. Mathew, N.R. Mathews, Phys. Status Solidi (A) 168 (1998) 177.
[25] A.Z. Wang, W.A. Anderson, M.A. Haase, J. Appl. Phys. 77 (7) (1995) 3513.
[26] M. Li, X. Zhen, L. Zhao, X. Chen, Advanced nanomaterials and nanodevices (IUMRS–ICEM 2002, Xi'an, China, June 10–14, 2002).
[27] G. Khlyap, M. Andrukhiv, Cryst. Res. Technol. 34 (5/6) (1999) 751.
[28] S.M. Sze, Semiconductor Devices, Physics and Technology, John Wiley & Sons, New York, 1985.
[29] A. Singh, P. Cova, J. Appl. Phys. 74 (1993) 6714.